



# *Trypanosoma cruzi* Induces the PARP1/AP-1 Pathway for Upregulation of Metalloproteinases and Transforming Growth Factor $\beta$ in Macrophages: Role in Cardiac Fibroblast Differentiation and Fibrosis in Chagas Disease

Subhadip Choudhuri,<sup>a</sup>  Nisha Jain Garg<sup>a,b</sup>

<sup>a</sup>Department of Microbiology and Immunology, University of Texas Medical Branch, Galveston, Texas, USA

<sup>b</sup>Institute for Human Infections and Immunity, University of Texas Medical Branch, Galveston, Texas, USA

**ABSTRACT** Chagas disease (CD), caused by *Trypanosoma cruzi*, is a degenerative heart condition. In the present study, we investigated the role of poly [ADP-ribose] polymerase 1/activator protein 1 (PARP1/AP-1) in upregulation of profibrotic macrophages (M $\phi$ ) and subsequent development of cardiac fibrosis in CD. We used *in vitro* and *in vivo* models of *T. cruzi* infection and chemical and genetic inhibition of *Parp1* to examine the molecular mechanisms by which M $\phi$  might augment profibrotic events in CD. Cultured (RAW 264.7 and THP-1) M $\phi$  infected with *T. cruzi* and primary cardiac and splenic M $\phi$  of chronically infected mice exhibited a significant increase in the expression, activity, and release of metalloproteinases (MMP2, MMP9, and MMP12) and the cytokine transforming growth factor  $\beta$  (TGF- $\beta$ ). M $\phi$  release of MMPs and TGF- $\beta$  signaled the cardiac fibroblast to myofibroblast differentiation, as evidenced by a shift from S100A4 to alpha smooth muscle actin ( $\alpha$ -SMA) expression. Incubation of infected M $\phi$  with MMP2 and MMP9 inhibitors resulted in 60 to 74% decline in TGF- $\beta$  release, and MMP9 and PARP1 inhibitors resulted in 57 to 70% decline in M $\phi$  TGF- $\beta$ -driven cardiac fibroblast differentiation. Likewise, histological studies showed a 12- to 16-fold increase in myocardial expression of CD68 (M $\phi$  marker) and its colocalization with MMP9/TGF- $\beta$ , galectin-3, and vimentin in wild-type mice with CD. In comparison, chronically infected *Parp1*<sup>-/-</sup> mice exhibited a >50% decline in myocardial levels of M $\phi$  and associated fibrosis markers. Further study showed that PARP1 synergized with c-Fos and JunB AP-1 family members for transcriptional activation of profibrotic response after *T. cruzi* infection. We conclude that PARP1 inhibition offers a potential therapy for controlling the *T. cruzi*-driven fibroblast differentiation in CD through modulation of the M $\phi$  signaling of the AP-1–MMP9–TGF- $\beta$  pathway.

**IMPORTANCE** Cardiomyopathy is the most important clinical manifestation of *T. cruzi*-driven CD. Recent studies have suggested the detrimental role of the matrix metalloproteinases MMP2 and MMP9 in extracellular matrix (ECM) degradation during cardiac remodeling in *T. cruzi* infection. Peripheral TGF- $\beta$  levels are increased in clinically symptomatic CD patients over those in clinically asymptomatic seropositive individuals. We provide the first evidence that during *T. cruzi* infection, M $\phi$  release of MMP2 and MMP9 plays an active role in activation of TGF- $\beta$  signaling of ECM remodeling and cardiac fibroblast-to-myofibroblast differentiation. We also determined that PARP1 signals c-Fos- and JunB-mediated AP-1 transcriptional activation of profibrotic gene expression and demonstrated the significance of PARP1 inhibition in controlling chronic fibrosis in Chagas disease. Our study provides a promising therapeutic approach for controlling *T. cruzi*-driven fibroblast differentiation in CD by

**Citation** Choudhuri S, Garg NJ. 2020. *Trypanosoma cruzi* induces the PARP1/AP-1 pathway for upregulation of metalloproteinases and transforming growth factor  $\beta$  in macrophages: role in cardiac fibroblast differentiation and fibrosis in Chagas disease. mBio 11:e01853-20. <https://doi.org/10.1128/mBio.01853-20>.

**Invited Editor** Daniel F. Hoft, Saint Louis University

**Editor** Anita A. Koshy, University of Arizona

**Copyright** © 2020 Choudhuri and Garg. This is an open-access article distributed under the terms of the [Creative Commons Attribution 4.0 International license](https://creativecommons.org/licenses/by/4.0/).

Address correspondence to Nisha Jain Garg, [nigarg@utmb.edu](mailto:nigarg@utmb.edu).

This article is a direct contribution from Nisha Jain Garg, a Fellow of the American Academy of Microbiology, who arranged for and secured reviews by Jyothi Nagajyothi, Hackensack University Medical Center, and Liwu Li, Virginia Tech.

**Received** 31 July 2020

**Accepted** 14 October 2020

**Published** 10 November 2020

PARP1 inhibitors through modulation of the M $\phi$  signaling of the AP-1–MMP9–TGF- $\beta$  pathway.

**KEYWORDS** Chagas disease, PARP1/AP-1, TGF- $\beta$ , *Trypanosoma cruzi*, cardiac fibrosis, metalloproteinases, profibrotic macrophages

Chagas disease (CD), also known as American trypanosomiasis, is caused by infection with the protozoan parasite *Trypanosoma cruzi*. *T. cruzi* is endemic to vast areas of the Western hemisphere, from Argentina to the southern parts of the United States. *T. cruzi*-infected individuals are found throughout the world due to their migration from areas of high *T. cruzi* endemicity to areas with relatively low insect transmission or no known insect transmission (reviewed in reference 1). Currently, CD affects 6 to 8 million people worldwide. Cardiomyopathy is the most important clinical manifestation of CD, affecting ~30% of the chronically infected individuals (2).

The pathology of CD is complex. Acute replication of *T. cruzi* in tissues is invariably associated with intense infiltration of mononuclear cells, including macrophages (M $\phi$ ), neutrophils, and lymphocytes, which are capable of controlling the parasite replication and dramatically decrease the number of parasitized cells (reviewed in references 3 and 4). However, the parasite is not eliminated by the innate and adaptive immune systems, and low-grade parasite persistence associated with ongoing inflammatory reactions causes scarring of the tissues and ultimately leads to gross cardiac pathology (2). The classic pathological features of chronic Chagas cardiomyopathy include low-grade myocarditis accompanied by myocytolysis, myofiber hypertrophy, and interstitial fibrosis (5). The chronic remodeling changes are often associated with a focal or diffused inflammatory infiltrate (6), though a causal relationship between specific types of cells in the inflammatory infiltrate and myocardial fibrosis and remodeling in chronic CD has not been established.

The extracellular matrix (ECM) network provides structural support to the heart. This network is mainly formed by thick fibers of type I collagen, which provide tensile strength, and thin fibers of type III collagen, which provide elasticity, and together these facilitate transmission of systolic force (7). In addition to collagens, glycoproteins, glycosaminoglycans (hyaluronan), and proteoglycans also form the cardiac ECM (8). Cardiac fibrosis is illustrated by net accumulation of ECM proteins in the myocardium and results in both systolic and diastolic dysfunctions (9). Though this process is not fully understood, it is conceivable that following injury by *T. cruzi* invasion and replication, activation of the latent growth factors, like transforming growth factor beta (TGF- $\beta$ 1 to - $\beta$ 3) and proteases in the cardiac ECM as well as in the tissue-resident and infiltrating M $\phi$  that phagocytize parasite and remove cell debris, can trigger a fibrotic response. As the dead cells and matrix are removed and the inflammatory response resolves with control of the parasite, an overall proliferative phase with replacement of cardiomyocytes with fibroblasts, myofibroblasts, and infiltration of other cells, resulting in cardiac remodeling, would ensue. Cellular and molecular pathways that contribute to ventricular remodeling, with presentation of hypertrophy initially and with apoptosis of fibroblasts and vascular and other cells, resulting in dilation of ventricles, are not fully understood in CD.

Recent studies have identified the role of matrix metalloproteinases (MMP2 and MMP9) in ECM degradation during cardiac remodeling in *T. cruzi* infection (reviewed in reference 10) and suggested that MMP2 and MMP9 together can be used to predict the clinical evolution of cardiac form of CD (11). There are many cell types, including the infiltrating neutrophils and cardiac tissue-resident M $\phi$ , that can produce MMPs; however, current literature has not addressed the role of M $\phi$  in signaling tissue fibrosis in progressive CD.

In this study, we aimed to evaluate whether acute or chronic *T. cruzi* infection induces M $\phi$  expression and release of active MMPs and whether M $\phi$  MMPs instigate profibrotic events in the heart. In this context, we investigated whether M $\phi$  TGF- $\beta$  activation is dependent on MMPs and causes fibroblasts to undergo myofibroblast

differentiation during *T. cruzi* infection and chronic disease development. We recently documented that PARP1 [poly(ADP-ribose) polymerase 1], through signaling NF- $\kappa$ B transcriptional activation, contributes to proinflammatory activation of M $\phi$  (12). We therefore also determined PARP1's role in regulation of M $\phi$  and cardiac fibrosis in CD. For this, we used cultured M $\phi$  and primary M $\phi$  isolated from bone marrow (BM) of wild-type (WT) and *Parp1*<sup>-/-</sup> mice and employed classical approaches to evaluate the PARP1 signaling of transcriptional programs relevant to profibrotic M $\phi$  response during *T. cruzi* infection.

## RESULTS

**Macrophages express and release MMPs in response to *T. cruzi* infection.** We first evaluated the mRNA levels for matrix metalloproteinases (MMPs) in RAW 264.7 M $\phi$  infected with *T. cruzi*. For this, M $\phi$  were incubated with *T. cruzi* (with or without gamma interferon [IFN- $\gamma$ ] and C-C motif chemokine ligand 2 [CCL2], individually or in combination) for 3 h and 18 h and analyzed by reverse transcription-quantitative PCR (RT-qPCR). We included IFN- $\gamma$  and CCL2 because these molecules are detected in the serum of infected mice and humans (13, 14), IFN- $\gamma$  is shown to regulate MMPs through suppression of the ATF-3/AP-1 transcription program in lipopolysaccharide (LPS)-treated M $\phi$  (15), while CCL2 is shown to enhance MMP9 expression (16). RAW M $\phi$  infected with *T. cruzi* (versus noninfected M $\phi$ ) exhibited 2.7- to 3.4-fold and 4.3- to 8.1-fold increases in mRNA levels for *Mmp2* and *Mmp9* (which encode gelatinases), respectively, and the maximal increase in *Mmp* mRNAs was observed at 18 h (Fig. 1A and B) ( $P < 0.001$ ). Further, we noted an 11.1-fold increase in mRNA for *Mmp12* (which encodes macrophage metalloelastase) at 18 h (Fig. 1C) ( $P < 0.001$ ) and a 2.3- to 5.5-fold increase in mRNA for *Mmp13* (which encodes collagenase 3) at 3 h and 18 h (Fig. S1A) ( $P < 0.001$ ). Coincubation with IFN- $\gamma$  and CCL2 had no significant effects on *T. cruzi*-induced mRNA levels for either of the MMPs at 3 h (Fig. 1A to C; Fig. S1A). At 18 h, IFN- $\gamma$  and CCL2 either had no effect or elicited 0.15- to 0.9-fold further increases in *Mmp2*, *Mmp9*, and *Mmp12* mRNA levels in infected M $\phi$  (Fig. 1A to C) ( $P < 0.05$ ). IFN- $\gamma$  and CCL2 had an overall suppressive effect on *T. cruzi*-induced increases in *Mmp13* mRNA in M $\phi$  (Fig. S1A) ( $P < 0.05$ ).

Western blot analysis and gelatin zymography were performed to assess the protein levels and activity of MMPs in infected M $\phi$ . Western blotting showed no significant changes in the intracellular levels of MMP2 or MMP9 in RAW M $\phi$  at 24 h postinfection (with or without IFN- $\gamma$  and CCL2) (Fig. 1D). Instead, spent medium of infected (versus noninfected) M $\phi$  at 24 h showed a 7- to 36-fold increase in MMP2 (66-kDa cleaved form)- and MMP9 (92 kDa)-mediated gelatin degradation (Fig. 1E and F) ( $P < 0.001$ ), determined by gelatin zymography. Coincubation with IFN- $\gamma$  and CCL2 for 24 h had nonsignificant effects on MMP2 release (Fig. 1F, panel a) and an overall suppressive effect on MMP9 release (Fig. 1F, panel b) ( $P < 0.001$ ) by M $\phi$  infected with *T. cruzi*. No increase in intracellular levels or release of active MMP2 and MMP9 by M $\phi$  was observed at 48 h postinfection.

MMP12 degrades soluble and insoluble elastin. We noted 2-fold and 9-fold increases in pro-MMP12 (54 kDa) and cleaved MMP12 (45 kDa) levels in cell lysates and spent medium, respectively, of infected (versus noninfected) M $\phi$  at 24 h (Fig. 1G and H) ( $P < 0.001$ ). Coincubation with IFN- $\gamma$  and CCL2 had nonsignificant or suppressive effects on *T. cruzi*-induced MMP12 levels at 24 h (Fig. 1G and H). By 48 h, intracellular levels of MMP12 were decreased in infected (with or without IFN- $\gamma$ ) M $\phi$ , while a 1.35-fold increase in secreted MMP12 was observed only when infected M $\phi$  were incubated with IFN- $\gamma$  and CCL2 (Fig. S1B and C). Together, the results presented in Fig. 1 and Fig. S1 suggest that *T. cruzi* infection of M $\phi$  elicits a significant increase in the expression of MMP2, MMP9, and MMP12 metalloproteinases that is predominantly independent of the presence of IFN- $\gamma$  and CCL2. Most of the MMP2 and MMP9 that exhibited gelatinase activity and the cleaved form of MMP12 were released from infected M $\phi$  within 24 h postinfection.

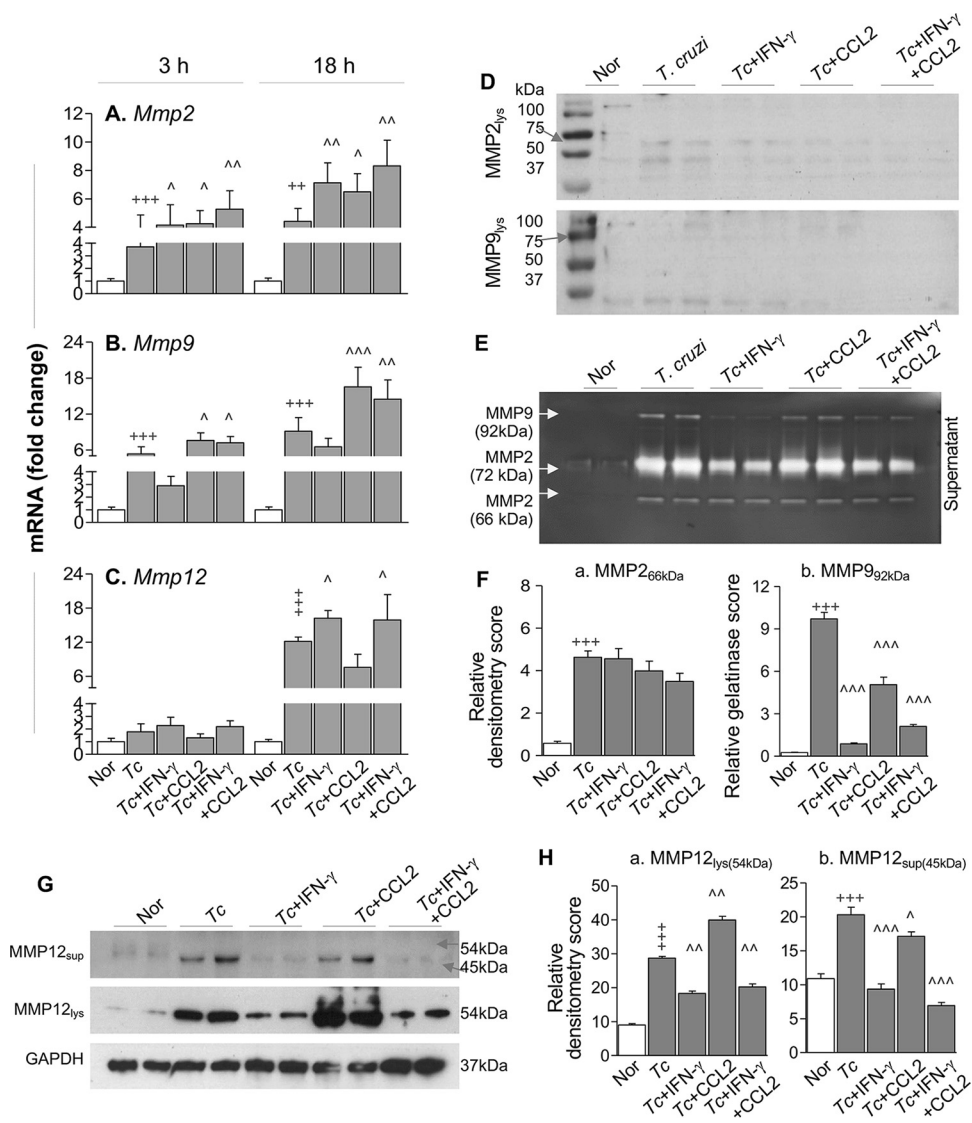


**FIG 1** Macrophages express and release metalloproteinases in response to *T. cruzi* infection. RAW 264.7 Mφ were incubated with medium or *T. cruzi* (*Tc*) trypomastigotes (cell-to-parasite ratio, 1:3) in the presence and absence of 20 ng/ml IFN-γ and 10 ng/ml CCL2 for 0 to 24 h. (A to C) Real-time RT-qPCR evaluation of mRNA levels for *Mmp2*, *Mmp9*, and *Mmp12* (normalized to *Gapdh*). (D) Western blot images for MMP2 and MMP9 in Mφ cell homogenates. Cells were incubated with *T. cruzi* trypomastigotes (cell-to-parasite ratio, 1:3) in the presence and absence of 20 ng/ml IFN-γ and 10 ng/ml CCL2 for 24 h. (E and F) Cell supernatants were collected after 24 h of incubation, concentrated 10-fold, and used for MMP2 (pro- form, 72 kDa; cleaved form, 66 kDa) and MMP9 (pro- form, 92 kDa) zymography. Bar graphs (F) show relative gelatin degradation scores. (G and H) Western blot images for MMP12 (pro- form, 54 kDa; cleaved form, 45 kDa [G]) and relative densitometry scores for MMP12 (normalized to GAPDH [H]) in cell homogenates and supernatants (obtained after 24 h of incubation). Data in bar graphs are means and SD and are representative of two independent experiments with two biological replicates per treatment per experiment (triplicate observations per sample for RT-qPCR analysis and duplicate observations per sample for gelatin zymography and Western blot analyses). Significance is annotated as follows: +, control versus infected (Student's two-tailed *t* test); ^, infected versus infected treated (one-way analysis of variance [ANOVA] followed by Tukey's *post hoc* correction test). ^,  $P \leq 0.05$ ; ++ and ^^,  $P \leq 0.01$ ; +++ and ^^,  $P \leq 0.001$ . Nor, normal (no infection).

**Macrophage production of metalloproteinases and TGF-β in Chagas disease.**

To verify our findings from *in vitro* studies (Fig. 1) and determine if profibrotic Mφ are stimulated in CD, we used a well-established mouse model of *T. cruzi* infection (17). Mice were euthanized at 150 days postinfection, which corresponds to the chronic disease phase. The splenic and cardiac CD11b<sup>+</sup> Mφ of infected and noninfected (control) mice were isolated and incubated for 24 h in complete medium, and cells and

supernatants were used for various studies. We detected 2.3-fold, 2.8-fold, and 8.1-fold increases in *Mmp2*, *Mmp9*, and *Tgfb1* mRNA levels, respectively, in splenic M $\phi$  of CD-infected (versus control) mice and 5.6-fold, 7.2-fold, and 9.7-fold increases in *Mmp2*, *Mmp9*, and *Tgfb1* mRNA levels, respectively, in myocardial M $\phi$  of chronically infected (versus noninfected) mice (Fig. 2A to C) ( $P < 0.001$ ). Splenic and cardiac M $\phi$  of Chagas (versus control) mice also exhibited 5- to 14.2-fold and 2.3- to 10.2-fold increases in TGF- $\beta$ , tumor necrosis factor alpha (TNF- $\alpha$ ), and monocyte-chemotactic protein 3 (MCP3) release, respectively, after 24 h of incubation (Fig. 2D to F) ( $P < 0.001$ ). Gelatin zymography showed 0.9-fold, 3.7-fold, and 4.0-fold increases in the gelatin degradation score for pro-MMP2 (72 kDa), cleaved MMP2 (66 kDa), and MMP9 (92 kDa), respectively, produced by splenic CD11b<sup>+</sup> M $\phi$  of chronically infected (versus noninfected) mice (Fig. 2G to J) ( $P < 0.001$ ). Likewise, we observed 12-fold, 6.1-fold, and 15.0-fold increase in the gelatin degradation score of pro-MMP2 and cleaved MMP2 and MMP9 (92 kDa), respectively, released by heart CD11b<sup>+</sup> M $\phi$  of chronically infected (versus noninfected) mice (Fig. 2G and H) ( $P < 0.001$ ). Together, these results show a profibrotic M $\phi$  response in chronic CD that is evidenced by an increase in the expression and release of active forms of MMP2 and MMP9 by splenic and heart M $\phi$  of CD-infected (versus noninfected) mice. The production of TGF- $\beta$  by splenic and heart M $\phi$  provides further support for their profibrotic role in CD.

**MMP2 and MMP9 promote TGF- $\beta$  activation in macrophages infected with *T. cruzi*.** MMP2 and MMP9 are (i) involved in degradation of ECM under normal physiologic and disease conditions (18), (ii) implicated in cell-to-cell communication independent of their ECM degradation function (19), and (iii) suggested to dock on the cell surface hyaluronic receptor CD44 to promote cleavage and activation of TGF- $\beta$  (20). TGF- $\beta$ , in turn, downregulates the inflammatory processes and activates cell-proliferative responses (18). To determine whether MMPs promote M $\phi$ 's profibrotic response by influencing TGF- $\beta$  during *T. cruzi* infection, we incubated RAW M $\phi$  with *T. cruzi* in the presence or absence of specific inhibitors of MMP2, MMP9, MMP12, and urokinase-type plasminogen activator (uPA) (which activates MMP2 and MMP9) and monitored release of TGF- $\beta$  and inflammatory cytokines/chemokines by an enzyme-linked immunosorbent assay (ELISA) at 24 h and 48 h. RAW M $\phi$  responded to *T. cruzi* infection with 9- to 10.5-fold, 20- to 27-fold, and 21- to 25-fold increases in TGF- $\beta$ , TNF- $\alpha$ , and MCP3/CCL7 release, respectively, at 24 h and 48 h post-incubation (Fig. 3A to C) ( $P < 0.001$ ). *T. cruzi*-induced TGF- $\beta$  production was decreased by 69 to 74%, 60 to 66%, and 79 to 82% when infected M $\phi$  were incubated with inhibitors of MMP2, MMP9, and uPA, respectively (Fig. 3A) ( $P < 0.001$ ). No effect of an MMP12 inhibitor on TGF- $\beta$  production by infected M $\phi$  was observed (Fig. 3A). Likewise, no effect of any of the metalloproteinase inhibitors was observed on *T. cruzi*-induced TNF- $\alpha$  and MCP3/CCL7 production by M $\phi$  at any of the time points studied (Fig. 3B and 3C). Together, these results suggest that (i) M $\phi$  respond to *T. cruzi* with a potent increase in profibrotic (TGF- $\beta$ ) and proinflammatory (TNF- $\alpha$  and MCP3) responses and (ii) M $\phi$  activation of TGF- $\beta$ , but not TNF- $\alpha$  and MCP3, was dependent on MMP2 and MMP9. Our observation of inhibitory effects of a uPA antagonist on TGF- $\beta$  production suggests that active forms of MMP2 and MMP9 signal TGF- $\beta$  activation in M $\phi$  infected by *T. cruzi*.

**M $\phi$  MMPs and TGF- $\beta$  contribute to cardiac fibroblast differentiation.** Cardiac fibroblast differentiation to myofibroblasts and ECM remodeling are the major drivers of cardiac fibrosis in Chagas and other heart diseases. To determine if *T. cruzi*-induced M $\phi$  production of gelatinases and TGF- $\beta$  stimulated cardiac fibroblast differentiation, we incubated human THP-1 M $\phi$  with *T. cruzi* in the presence and absence of inhibitors of MMP2 and MMP9 for 24 h and collected the supernatants. Next, human cardiac fibroblasts (HCF) were incubated for 48 h, 72 h, and 96 h with spent medium from infected M $\phi$  and subjected to immunostaining using fluorescence-tagged antibodies against S100A4 (fibroblast-specific) and alpha smooth muscle actin ( $\alpha$ -SMA) (myofibroblast-specific) proteins. HCF incubated with medium from *T. cruzi*-infected M $\phi$  exhibited a significant differentiation to myofibroblasts, as evidenced by a gradual increase in the

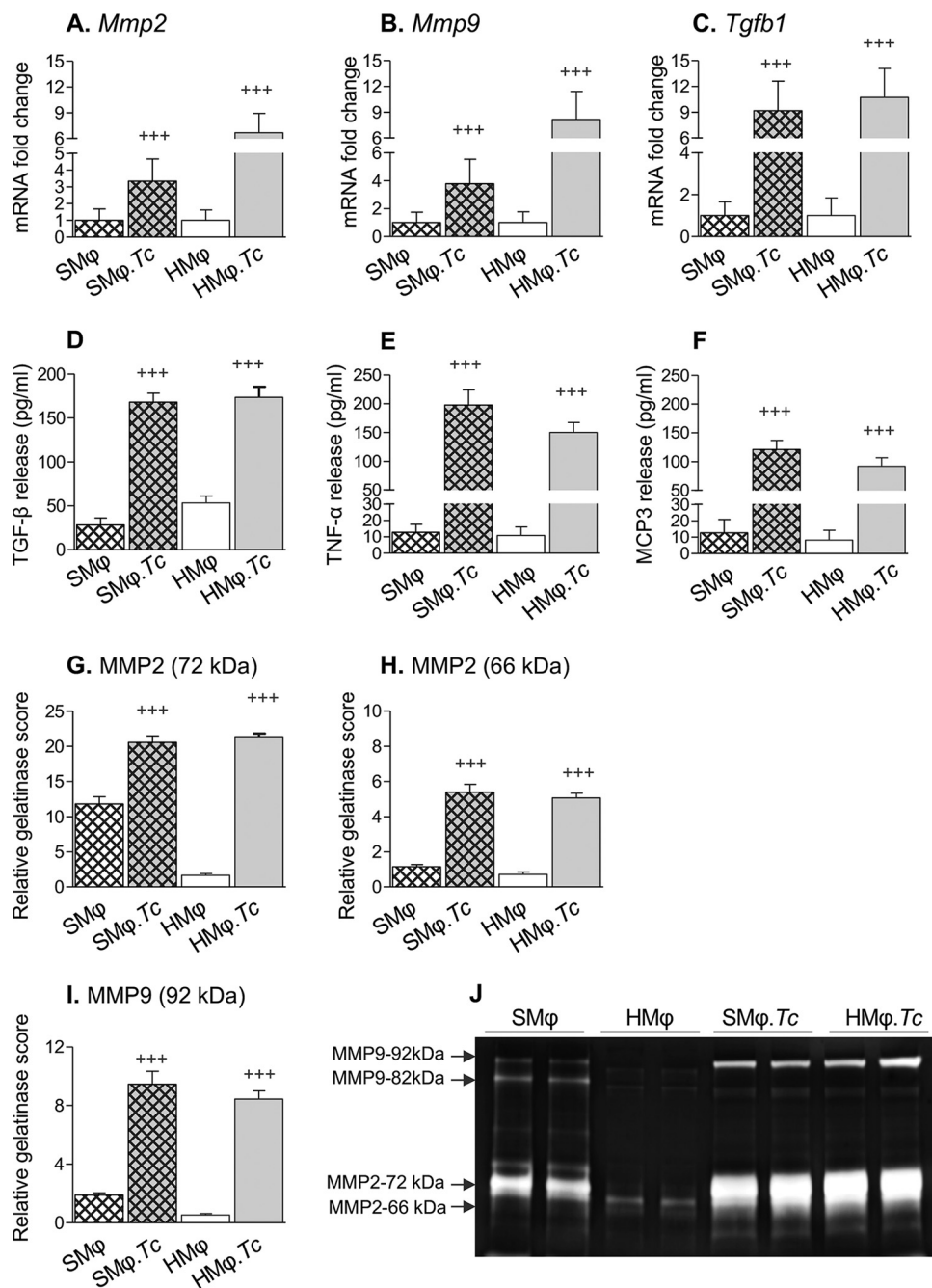


**FIG 2** Profibrotic response of splenic and cardiac macrophages in CD-infected mice. Mice were infected with *T. cruzi* (10,000 parasites per mouse) and euthanized at 150 days postinfection (controls had no infection). Spleen (SM $\phi$ ) and heart (HM $\phi$ ) macrophages were isolated using CD11b<sup>+</sup> magnetic beads and incubated *in vitro* for 24 h. (A to C) Real-time RT-qPCR evaluation of mRNA levels. (D to F) TGF- $\beta$ , TNF- $\alpha$ , and MCP3 release in supernatants, determined by an ELISA. (G to J) Gelatin zymography for MMP2 and MMP9 in culture supernatants of splenic and heart M $\phi$  (J) and relative gelatin degradation scores for pro-MMP2 (G), cleaved MMP2 (H), and pro-MMP9 (I). Data (means and standard deviation [SD]) are representative of two independent experiments with two biological replicates per treatment (triplicate and duplicate observations per sample for RT-qPCR and zymography, respectively). Significance was calculated by Student's two-tailed *t* test or a nonparametric Mann-Whitney U test. + + +,  $P \leq 0.001$ .

frequency of  $\alpha$ -SMA<sup>+</sup> cells from 10% to 82% and a decline in the frequency of S100A4<sup>+</sup> cells from 89% to 17% during 48 to 96 h of incubation (Fig. 4E to H). These findings were consistent with the observations made using recombinant TGF- $\beta$ 1 that also led to a gradual increase in the frequency of  $\alpha$ -SMA<sup>+</sup> cells from 12% to 93% with a corre-

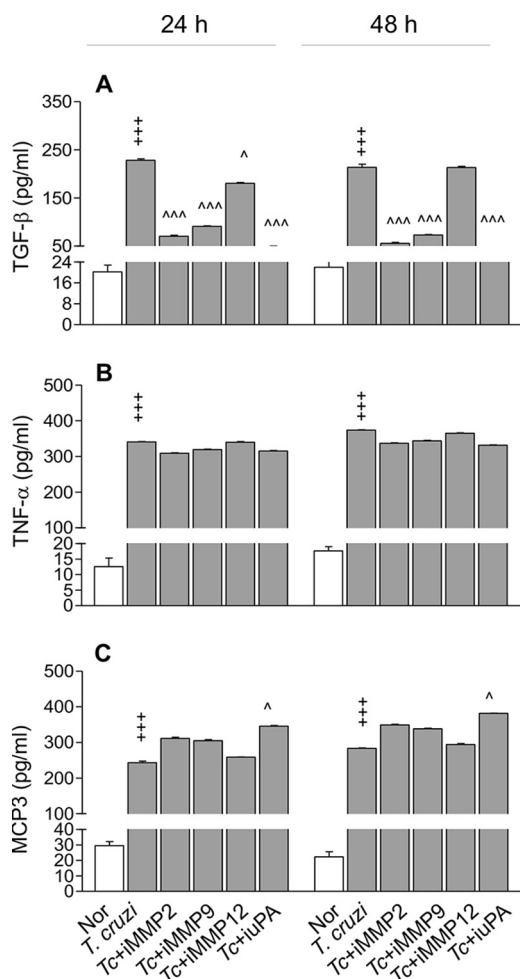


**FIG 3** MMP2 and MMP9 are required for TGF- $\beta$  production by M $\phi$  in response to *T. cruzi* infection. RAW 264.7 M $\phi$  were incubated with *T. cruzi* trypomastigotes in the presence and absence of 10  $\mu$ M ARP-100 (which inhibits MMP2), 10  $\mu$ M MMP9 inhibitor-1 (which inhibits MMP9), 10  $\mu$ M MMP408 (which inhibits MMP12), or 10  $\mu$ M uk122 (which inhibits urokinase-type plasminogen activator [uPA]). Cell culture supernatants were used for the detection of TGF- $\beta$  (A), TNF- $\alpha$  (B), and MCP3/CCL7 (C) by an ELISA. Data are representative of two independent experiments (three biological replicates per treatment and duplicate observations per sample) and are means and SD. ^,  $P \leq 0.05$ ; +++ and ^^,  $P \leq 0.001$  (+, noninfected versus infected by Student's two-tailed *t* test or nonparametric Mann-Whitney U test; ^, infected versus infected/reated by one-way ANOVA and Tukey's *post hoc* test).

sponding decline in the frequency of S100A4<sup>+</sup> cells from 87% to 7% during 48 to 96 h of incubation (Fig. 4Q to T). In comparison, incubation of HCF with spent medium from noninfected M $\phi$  resulted in no differentiation (Fig. 4A to D). When incubated with supernatants from THP-1 M $\phi$  previously treated with *T. cruzi* and an MMP2 antagonist, HCF continued to exhibit up to 67% differentiation to an  $\alpha$ -SMA<sup>+</sup> phenotype by 96 h (Fig. 4I to L), which indicates that MMP2 has a less significant impact on cardiac fibroblast-to-myofibroblast differentiation. In contrast, incubation of HCF with supernatant of THP-1 M $\phi$  previously treated with *T. cruzi* and an MMP9 antagonist led to only a 30% increase in the frequency of  $\alpha$ -SMA<sup>+</sup> cells, while up to 70% of the cells retained the S100A4-positive phenotype during the 96 h (Fig. 4M to P). Together, the results presented in Fig. 4, along with those in Fig. 3, suggest that MMP9 plays a key role in the release of functional TGF- $\beta$ 1 by M $\phi$  infected by *T. cruzi*, and M $\phi$  release of MMP9/TGF- $\beta$  creates a microenvironment conducive to differentiation of cardiac fibroblasts to myofibroblasts.

**PARP1 signaling of profibrotic response during *T. cruzi* infection and Chagas disease.** We have reported that PARP1 plays a regulatory role in signaling the NF- $\kappa$ B-

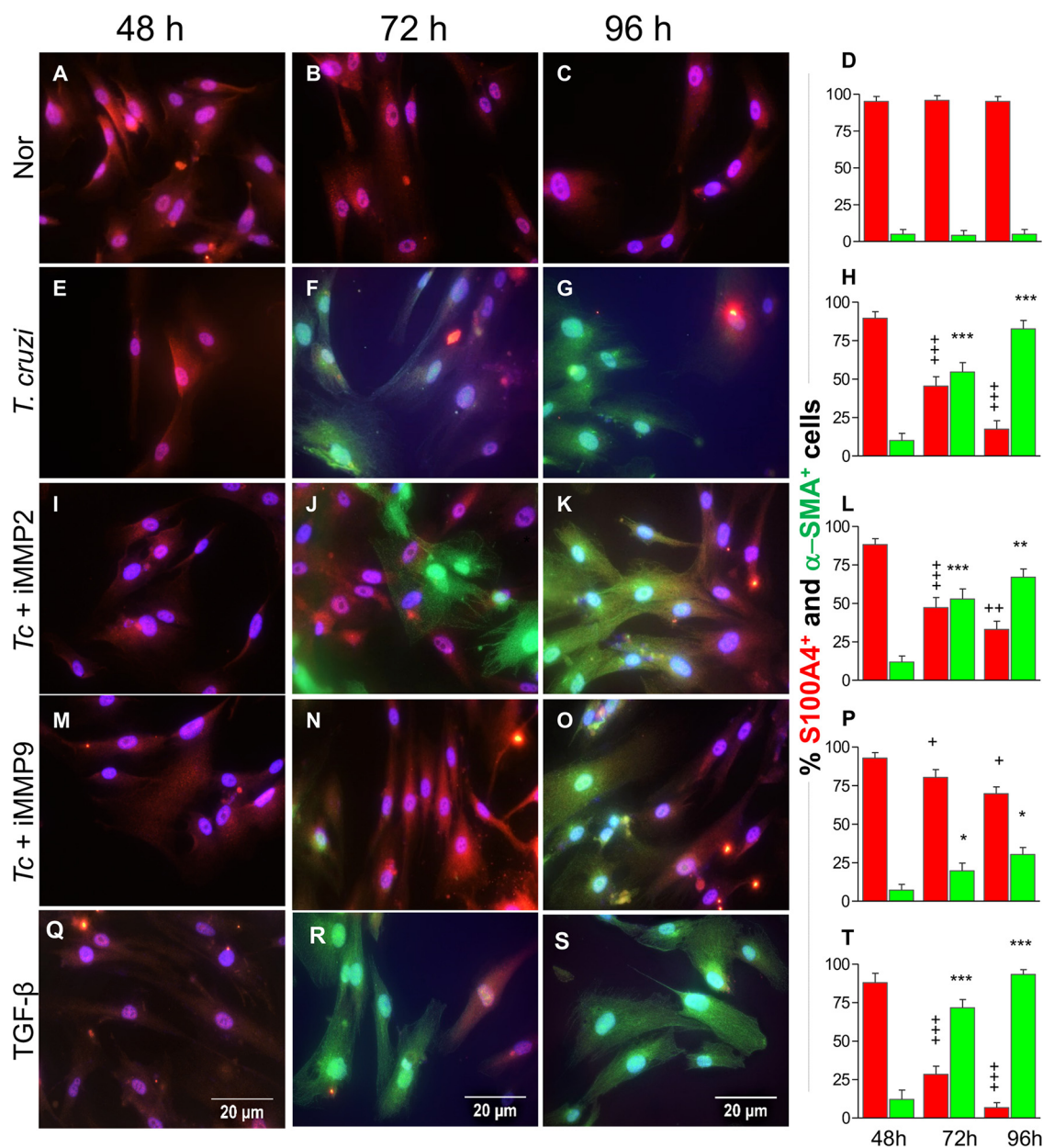


**FIG 4** Inhibition of Mφ MMP9 arrests TGF-β-dependent cardiac fibroblast transition to myofibroblasts in response to *T. cruzi*. Human THP-1 Mφ were incubated for 24 h with *T. cruzi* in the presence or absence of 10 μM concentrations of inhibitors of MMP2 or MMP9. Next, human cardiac fibroblast (HCF) cells were incubated for 48 to 96 h with spent medium from THP-1 Mφ that were noninfected (A to D), infected (E to H), or infected and treated with inhibitors of MMP2 (I to L) or MMP9 (M to P). Positive controls were HCF cells incubated with recombinant TGF-β (Q to T). Transition of HCF to myofibroblasts was determined by immunofluorescence staining for S100A4 (red) and α-SMA (green), respectively. DAPI (4',6-diamidino-2-phenylindole; blue) staining marks nuclei. Representative images are shown at a magnification of ×40. Bar graphs show percentages of S100A4<sup>+</sup> and α-SMA<sup>+</sup> HCF at 48 to 96 h post-incubation. Data (means and SD) are derived from two independent experiments, with three biological replicates per treatment, and each sample was analyzed in 9 microscopic fields. Significance comparing the expression of S100A4 (+) or α-SMA (\*) at different time points was calculated by repeated-measures ANOVA or *post hoc* test. + and \*,  $P \leq 0.05$ ; ++ and \*\*,  $P \leq 0.01$ ; +++ and \*\*\*,  $P \leq 0.001$ .

mediated proinflammatory gene expression in cardiac myocytes and Mφ in response to *T. cruzi* infection (12, 21) and in Mφ stimulated with extracellular vesicles (EV) released by infected cells (12). Since NF-κB can be involved in transcription of metalloproteinases, we determined if PARP1 also signals profibrotic gene expression during *T. cruzi* infection. For this, we incubated RAW Mφ with *T. cruzi* in the presence or absence of 10 μM iniparib (a selective PARP1 inhibitor) for 24 h and performed RT-qPCR analysis. We also incubated Mφ with *T. cruzi*-induced EV (TEV) previously purified from the

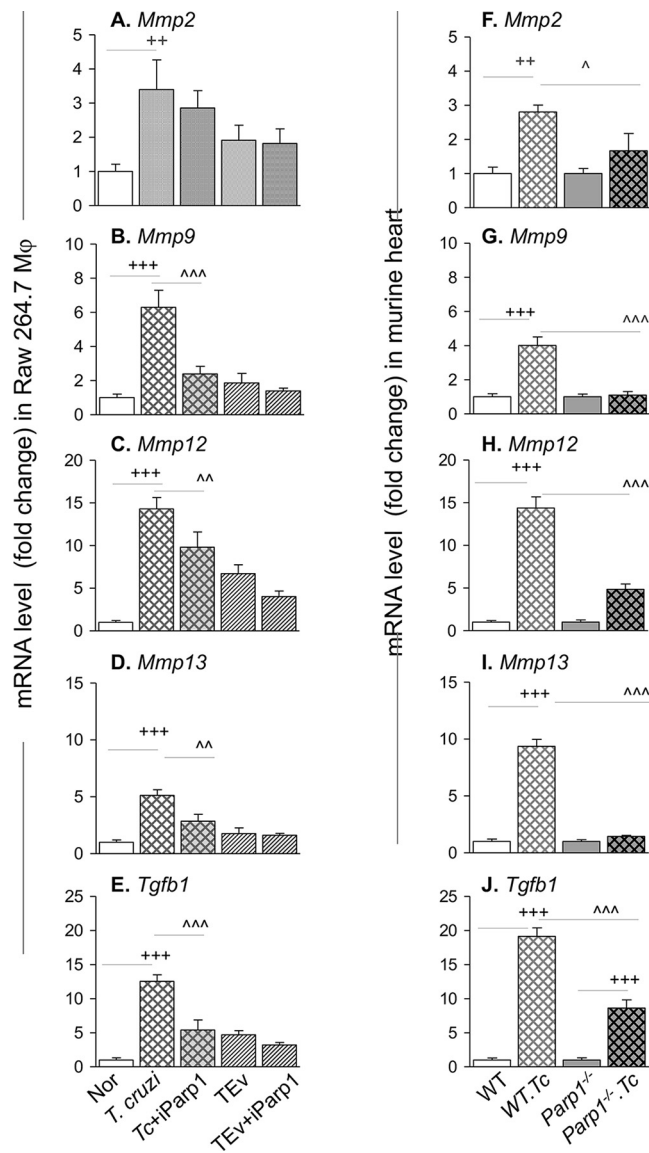


**FIG 5** MMP and TGF- $\beta$  expression in response to *T. cruzi* infection is PARP1 dependent. (A to E) RAW 264.7 M $\phi$  were incubated with *T. cruzi* for 72 h and extracellular vesicles (EV) released in supernatants were isolated. Next, a new batch of M $\phi$  was incubated for 18 h with *T. cruzi* or *T. cruzi*-induced EV (TEV) in the presence or absence of 10  $\mu$ M iniparib (which inhibits PARP1). The mRNA levels for *Mmp2*, *Mmp9*, *Mmp12*, *Mmp13*, and *Tgfb1*, normalized to *Gapdh*, were measured by real-time RT-qPCR. (F to J) RT-qPCR evaluation of mRNAs in heart tissue of WT and *Parp1*<sup>-/-</sup> mice euthanized at 150 days postinfection (controls had no infection). Data are representative of two independent experiments with 3 biological replicates per treatment (triplicate observations per sample). Significance is annotated as follows: +, noninfected versus infected; ^, infected versus infected with chemical or genetic deletion of PARP1 (Student's two-tailed *t* test or nonparametric Mann-Whitney U test). ^,  $P \leq 0.05$ ; ++ and ^^,  $P \leq 0.01$ ; +++ and ^^,  $P \leq 0.001$ . iParp1, inhibitor of PARP1.

culture supernatants of *T. cruzi*-infected M $\phi$ . As expected from the data in Fig. 2, M $\phi$  infected with *T. cruzi* (versus noninfected) showed 2.5-fold, 5.3-fold, 13.3-fold, 4.1-fold, and 12.5-fold increases in the mRNA levels for *Mmp2*, *Mmp9*, *Mmp12*, *Mmp13*, and *Tgfb1*, respectively (Fig. 5A to E) ( $P < 0.001$ ). Coincubation with a PARP1 inhibitor resulted in 16%, 62%, 32%, 44%, and 57% declines in *T. cruzi*-induced *Mmp2*, *Mmp9*, *Mmp12*, *Mmp13*, and *Tgfb1* mRNA levels, respectively, in infected M $\phi$  (Fig. 5A to E) ( $P < 0.01$ ). PARP1 was also required for driving the cardiac fibroblast differentiation to myofibroblasts. This was evidenced by the findings that HCF cells incubated for 96 h with supernatants of THP-1 M $\phi$  previously incubated with *T. cruzi* and PARP1 inhibitor

exhibited only a 43% increase in the frequency of  $\alpha$ -SMA<sup>+</sup> cells (Fig. S2A to D). In comparison, up to 83% of the HCF had gained the  $\alpha$ -SMA<sup>+</sup> phenotype when incubated with supernatants of THP-1 M $\phi$  previously incubated with *T. cruzi* only (Fig. 4E to H). We observed no changes in *Mmp3* and *Mmp8* mRNA levels in M $\phi$  incubated with *T. cruzi* (with or without PARP1 inhibitor) (Fig. S2E and F) compared to matched controls. Likewise, incubation with TEV (with or without PARP1 inhibitor) resulted in no significant increase in mRNA expression for any of the metalloproteinases and TGF- $\beta$  compared to that noted in normal controls (Fig. 5A to E; Fig. S2E and F).

We also examined the *in vivo* effects of PARP1 on the profibrotic gene expression profile in CD. These data showed 1.8-fold, 3-fold, 13.3-fold, 8.3-fold, and 18-fold increases in mRNA levels for *Mmp2*, *Mmp9*, *Mmp12*, *Mmp13*, and *Tgfb1*, respectively, in the heart tissues of chronically infected (versus noninfected) WT mice (Fig. 5F to J) ( $P < 0.01$ ). Interestingly, chronically infected *Parp1*<sup>-/-</sup> mice, in comparison to infected WT mice, exhibited 42%, 72%, 66%, 85%, and 57% declines in mRNA levels for *Mmp2*, *Mmp9*, *Mmp12*, *Mmp13*, and *Tgfb1*, respectively (Fig. 5F to J) ( $P < 0.05$ ). We observed no changes in *Mmp3* and *Mmp8* mRNA levels in the heart tissues of chronically infected WT or *Parp1*<sup>-/-</sup> mice (Fig. S2G and H) compared to matched controls.

Together, the results presented in Fig. 5 and Fig. S2 suggest that (i) PARP1 is required to activate the profibrotic transcriptional profile in M $\phi$  infected by *T. cruzi* and in heart tissues of Chagas mice and (ii) chemical inhibition or genetic deletion of *Parp1* was beneficial in arresting M $\phi$  profibrotic gene expression and consequently TGF- $\beta$ -driven cardiac fibroblast-to-myofibroblast differentiation in response to *T. cruzi* infection.

**Tissue infiltration of profibrotic macrophages in Chagas mice (with and without PARP1).** Next, we focused on determining the *in vivo* role of PARP1 and M $\phi$  in driving cardiac fibrosis by immunohistochemical staining of the heart tissue sections of chronically infected (and control) mice (Fig. 6). Semiquantitative scoring of immunostaining data showed that myocardial infiltration of CD68<sup>+</sup> (classical M $\phi$  marker) cells was increased by 13-fold and 5.5-fold in chronically infected WT and *Parp1*<sup>-/-</sup> (versus matched control) mice, respectively (Fig. S3) ( $P < 0.001$ ). Myocardial frequencies of MMP9<sup>+</sup> and CD68<sup>+</sup> MMP9<sup>+</sup> cells were increased by 6-fold and 12-fold, respectively, in WT *T. cruzi*-infected (versus noninfected) mice (compare Fig. 6A with Fig. 6B, E, and F), whereas *Parp1*<sup>-/-</sup> *T. cruzi*-infected (versus WT *T. cruzi*-infected) mice exhibited a 45 to 50% decline in myocardial MMP9<sup>+</sup> and CD68<sup>+</sup> MMP9<sup>+</sup> staining (compare Fig. 6B with Fig. 6D, E, and F) ( $P < 0.001$ ). Likewise, we observed in WT *T. cruzi*-infected (versus noninfected) mice 4.8- to 5.4-fold increases in myocardial frequency of TGF- $\beta$ <sup>+</sup> (Fig. 6G, H and K), galectin-3<sup>+</sup> (Fig. 6M, N and Q), and vimentin<sup>+</sup> (Fig. 6S, T and W) signal and 14- to 16-fold increases in colocalization of these molecules with CD68, which indicated the role of M $\phi$  in driving the profibrotic (CD68<sup>+</sup> TGF- $\beta$ <sup>+</sup>) (Fig. 6L), fibrotic (CD68<sup>+</sup> galectin-3<sup>+</sup>) (Fig. 6R), and fibroblast-to-myofibroblast differentiation (CD68<sup>+</sup> vimentin<sup>+</sup>) profiles in CD (Fig. 6X) ( $P < 0.001$  for all). In comparison to WT *T. cruzi*-infected mice, chronically infected *Parp1*<sup>-/-</sup> mice exhibited a 68 to 73% decline in TGF- $\beta$ <sup>+</sup>, galectin-3<sup>+</sup>, and vimentin<sup>+</sup> myocardial staining and a 65 to 70% decline in CD68<sup>+</sup> TGF- $\beta$ <sup>+</sup>, CD68<sup>+</sup> galectin-3<sup>+</sup>, and CD68<sup>+</sup> vimentin<sup>+</sup> colocalization staining (Fig. 6G to X) ( $P < 0.001$ ). These results suggest that PARP1 regulates myocardial profibrotic response in chronic Chagas disease and that PARP1 depletion is beneficial in arresting M $\phi$  MMP9/TGF- $\beta$ -driven cardiac fibroblast differentiation to myofibroblasts and tissue fibrosis in chronic Chagas disease-affected hearts.

**Transcriptional activation of profibrotic gene expression in M $\phi$  infected by *T. cruzi* (with or without PARP1).** Finally, we examined transcriptional regulation of metalloproteinases in M $\phi$ . Genome-wide studies have identified transcription binding sites for activator protein 1 (AP-1), AP-2, NF- $\kappa$ B, RUNX-2, and STAT-3 in promoter sequences of genes encoding metalloproteinases, especially MMP2 and MMP9, and TGF- $\beta$  (22). To determine which of these transcription factors might be involved in upregulation of the profibrotic response to *T. cruzi*, we infected RAW M $\phi$  with *T. cruzi*, incubated them in the presence and absence of specific antagonists of transcription

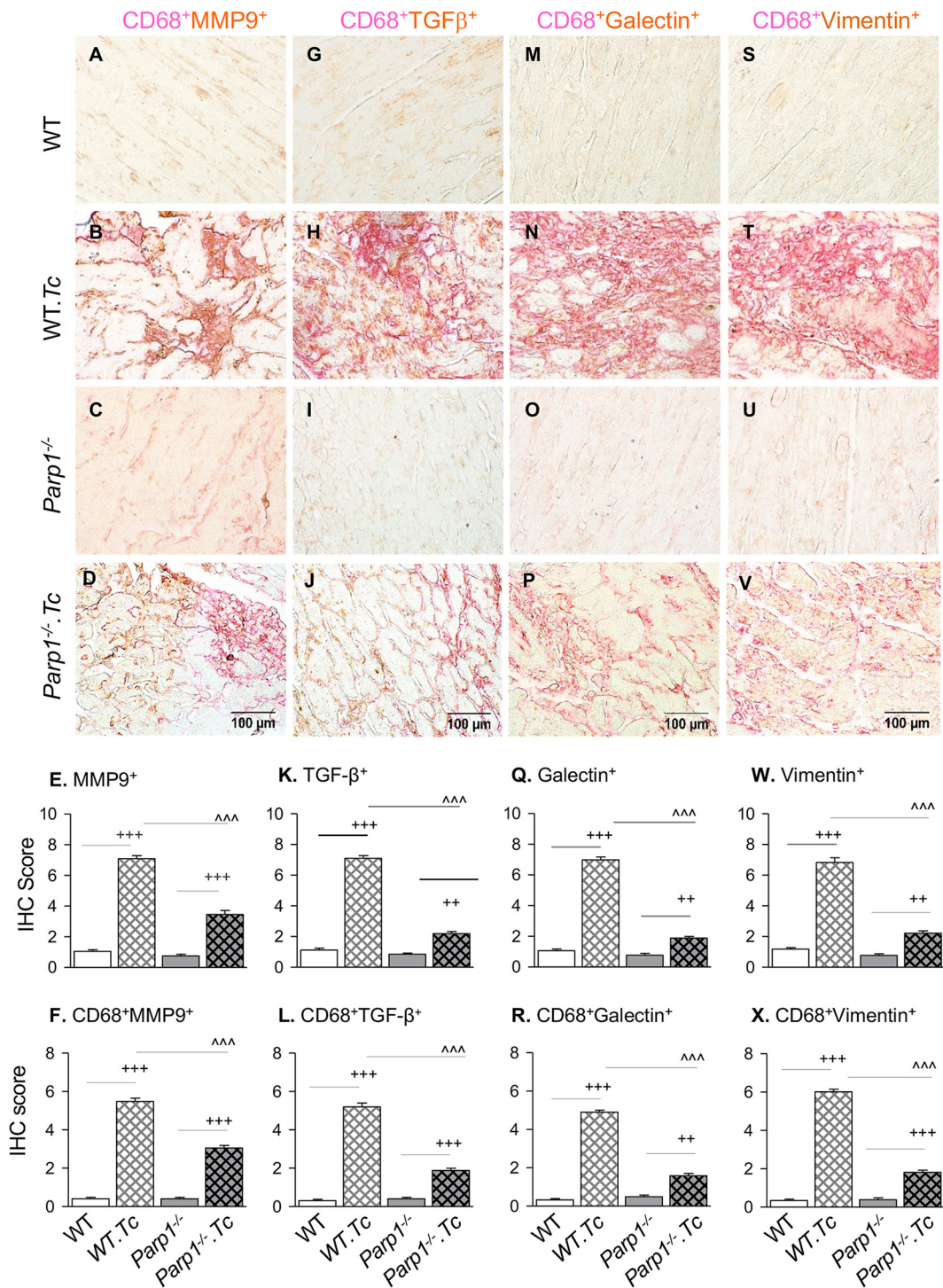


**FIG 6** Profibrotic macrophages and tissue fibrosis in myocardium of CD-infected mice (with and without PARP1). Mice (WT and *Parp1*<sup>-/-</sup>) were challenged with *T. cruzi* and euthanized at 150 days postinfection. Paraffin-embedded left ventricular tissue sections were subjected to immunohistochemical staining. Representative images show colocalization of CD68 (magenta, Mφ marker) with MMP9 (A to D), TGF-β (G to J), galectin (M to P), and vimentin (S to V) (magnification, ×60). Semiquantitative immunohistochemistry scores for tissue levels of MMP9, TGF-β, galectin, and vimentin (E, K, Q, and W, respectively) and CD68<sup>+</sup> Mφ colocalized with MMP9, TGF-β, galectin, and vimentin (F, L, R, and X, respectively) are shown. Bar graphs show means and SD (3 mice per group, two tissue sections per mouse, 9 microscopic fields per tissue section; magnification, ×20). Significance was calculated by Student's two-tailed *t* test or nonparametric Mann-Whitney *U* *t* test and is annotated as follows: +, WT versus WT *T. cruzi*-infected or *Parp1*<sup>-/-</sup> *T. cruzi*-infected; ^, WT *T. cruzi*-infected versus *Parp1*<sup>-/-</sup> *T. cruzi*-infected. ++, *P* ≤ 0.01; +++ and ^^^, *P* < 0.001).

factors, and monitored gene expression by RT-qPCR at 3 h and 24 h. *T. cruzi* induced a 3- to 7-fold increase in *Mmp2*, *Mmp9*, and *Tgfb1* mRNA levels that was not significantly changed in the presence of any of the inhibitors at 3 h (Fig. 7A to C). By 24 h, we noted an 8- to 20-fold increase in *Mmp2*, *Mmp9*, and *Tgfb1* mRNA levels in infected (versus control) M $\phi$  (Fig. 7A to C). Coincubation with an AP-1 inhibitor resulted in 52%, 66.5%, and 68% declines in *T. cruzi*-induced *Mmp2*, *Mmp9*, and *Tgfb1* mRNAs, respectively ( $P < 0.001$  for all), while NF- $\kappa$ B inhibition resulted in a 45 to 50% decline in *Mmp2* and *Mmp9* mRNAs ( $P < 0.001$ ) but had no effect on *T. cruzi*-induced increases in *Tgfb1* mRNA levels in infected M $\phi$  (Fig. 7A to C). Furthermore, inhibition of RUNX2 and STAT3 transcription factors had no effect on the mRNA levels of *Mmp2*, *Mmp9*, or *Tgfb1* in infected M $\phi$ . These results suggest that AP-1 is involved primarily in transcriptional activation of the profibrotic response in M $\phi$  infected by *T. cruzi*.

PARP1 is shown to activate JNK and DNA binding of AP-1 in fibroblasts (23) and enhance NF- $\kappa$ B/AP-1 binding to MMP9 promoter sequence in diabetic retinopathy (24), though its role in transcriptional activation of the profibrotic program in M $\phi$ , if any, is not known. To investigate whether PARP1 is engaged in AP-1 transcriptional activation of the profibrotic response, we incubated the primary bone marrow M $\phi$  of WT and *Parp1*<sup>-/-</sup> mice with *T. cruzi* trypomastigotes for 24 h and utilized the nuclear extracts for an AP-1 transcription factor family assay. We found 2.64-fold, 2.86-fold, and 0.65-fold increases in c-Fos, JunB, and c-Jun AP-1 family proteins, respectively, in primary WT M $\phi$  infected with *T. cruzi* (versus no infection;  $P < 0.001$ ) (Fig. 7D, G, and I). *Parp1*<sup>-/-</sup> M $\phi$  infected with *T. cruzi* exhibited 1.3-fold and 1.5-fold declines in c-Fos and JunB levels, respectively (Fig. 7D and 7G) ( $P < 0.001$ ), but no decline in c-Jun level (Fig. 7I) compared to infected WT M $\phi$ . No activation of FosB, Fra-1, or JunD AP1 transcriptional family proteins was observed in either the WT or *Parp1*<sup>-/-</sup> primary M $\phi$  in response to *T. cruzi* infection (Fig. 7E, F, and H). Together, the results presented in Fig. 7 suggest that PARP1 signals transcriptional activation of c-Fos and JunB AP-1 transcriptional family proteins to regulate the M $\phi$  profibrotic response to *T. cruzi* infection and CD.

## DISCUSSION

There is a growing body of research endorsing the role of parasite persistence in facilitating the myocardial infiltration of immune and nonimmune cells and disturbing cardiac homeostasis (reviewed in reference 2). Dilated cardiomyopathy, the pathological manifestation of chronic CD, is characterized by diffused myocarditis, ECM remodeling, and interstitial fibrosis, which cause left ventricular dysfunction (5, 6). Matrix metalloproteinases, especially MMP2 and MMP9, have emerged as modulators of cardiovascular inflammation as well as remodeling. In acute *T. cruzi* infection, MMP2 and MMP9 expression was associated with increased inflammation, and treatment with MMP2/MMP9 antagonists was beneficial in controlling inflammatory pathology and mortality in mice (25). In chronic CD, increased plasma levels of MMP2 predicted early cardiac remodeling in clinically asymptomatic CD, while MMP9 was identified as a risk factor for late fibrosis and severe cardiac remodeling in clinically symptomatic patients (11). By using flow cytometry evaluation of peripheral blood cells, Medeiros et al. (26) showed that intracellular MMP2 and MMP9 levels were increased in neutrophils and monocytes of seropositive patients. When cells were exposed to a *T. cruzi* antigenic stimulus, the frequency of MMP2- and MMP9-expressing monocytes was further increased in peripheral blood cells of clinically symptomatic patients with the cardiac form of the disease but not in the seropositive, clinically asymptomatic individuals, thus implying that immune cells may contribute to fibrosis in CD through MMP production. In the present study, we demonstrate that expression and activity of MMP2, MMP9, and MMP12 were increased in cultured and primary (splenic and cardiac) M $\phi$  in response to *T. cruzi* infection and in the myocardium of chronically infected mice (Fig. 1 and 2). The M $\phi$  activation of metalloproteinases by *T. cruzi* was not critically influenced by CCL2 and IFN- $\gamma$ , as is observed in other disease models (27–29). Furthermore, *T. cruzi*-induced M $\phi$  metalloproteinases (MMP9 more than MMP2) promoted TGF- $\beta$  production and human cardiac fibroblast-to-myofibroblast differentiation *in vitro* (Fig. 4). The MMP2-

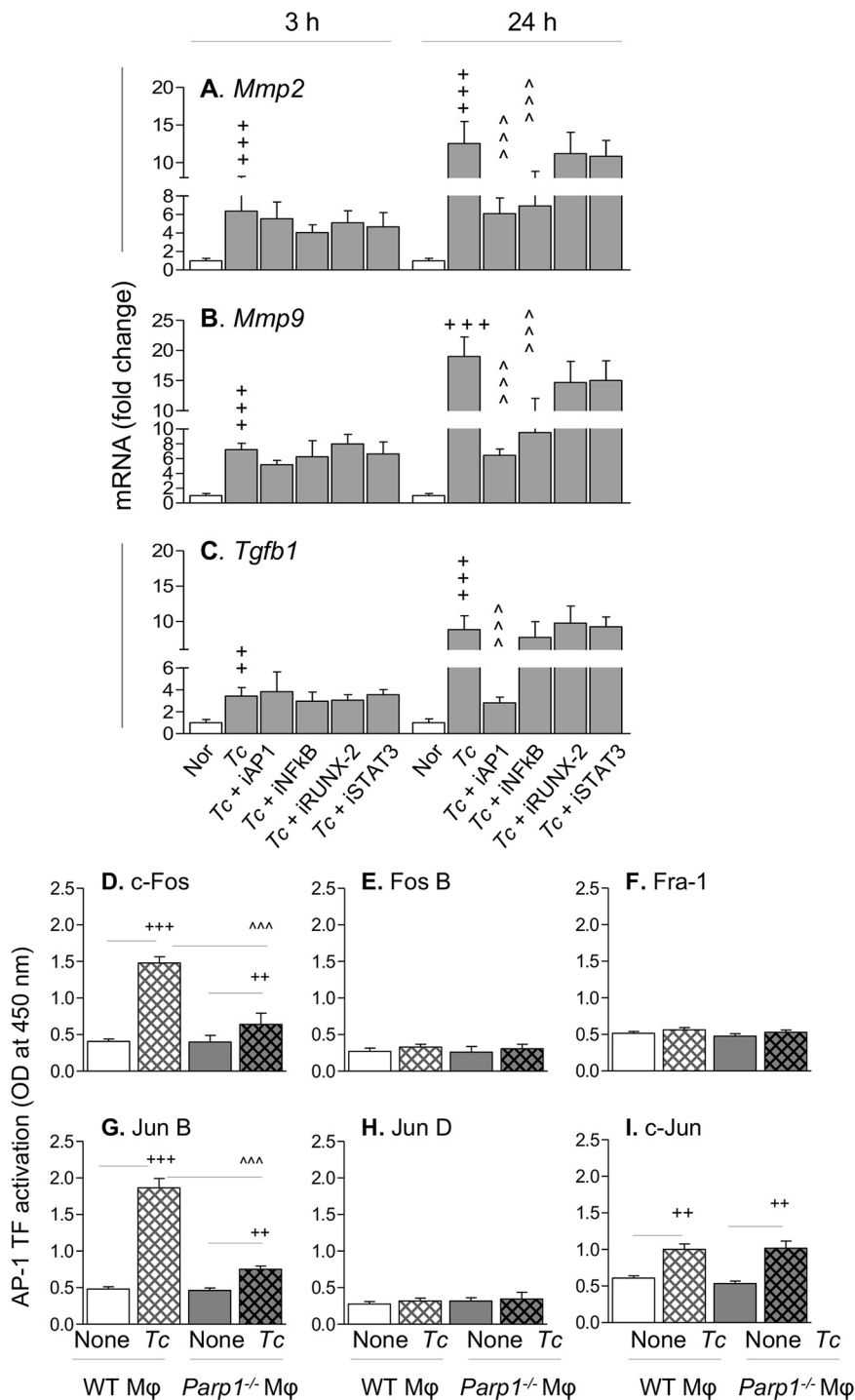


**FIG 7** PARP1 induces *T. cruzi*-mediated fibrotic response through transcriptional activation of AP-1. (A to C) RAW 264.7 Mφ were incubated with *T. cruzi* in the presence and absence of 10 μM concentrations of specific inhibitors of NF-κB, AP-1, RUNX-2, and STAT3. Results of real-time RT-qPCR for *Mmp2*, *Mmp9*, and *Tgfb1* (normalized to *Gapdh*) are shown. (D to I) BM-derived primary Mφ were infected with *T. cruzi* for 24 h, and nuclear fractions were used to evaluate c-Fos (D), Fos B (E), Fra-1 (F), JunB (G), JunD (H), and c-Jun (I) by using AP-1 transcription factor family ELISA. Data (means and SD) are representative of two independent experiments, 2 or 3 biological replicates per treatment, and 2 or 3 observations per sample. Significance is annotated as follows: +, noninfected versus infected (Student's two-tailed *t* test or nonparametric Mann-Whitney U test); ^, infected versus infected and treated (one-way ANOVA followed by Tukey's *post hoc* correction test). ++, *P* ≤ 0.01; +++, and ^^^, *P* ≤ 0.001).

and MMP9-producing M $\phi$  were also associated with myocardial fibrosis, which presented with increased tissue distribution of TGF- $\beta$  (which indicates a profibrotic response), galectin-3 (a marker of fibrotic response), and vimentin (a marker of fibroblast differentiation to myofibroblasts) in chronically infected Chagas mice (Fig. 6). Our findings endorse the importance of cardiac M $\phi$  in driving the MMP2/MMP9-mediated, TGF- $\beta$ -dependent profibrotic-fibrotic outcomes in the heart during *T. cruzi* infection and CD development.

The M $\phi$ -specific matrix metalloproteinase, i.e., MMP12, is identified as an endogenous resolution promoting factor in the events of myocardial infarction (30), and it plays a protective role by arresting inflammatory pathways and neutrophil infiltration in various diseases (31). MMP13 is a member of the collagenase family, which degrades many types of collagens and other profibrotic molecules (32). *In vitro* studies have identified many chemokines (e.g., CCL2, -3, -5, -7, -8, -15, -16, -17, and -23) as putative MMP13 substrates (33). Studies in *Mmp13*-deficient mice have identified contradictory phenotypes, with finding of attenuated inflammation and pulmonary fibrosis after irradiation-induced injury (34), no effect on fibrotic responses and an increase in inflammatory profile after hypertoxic lung injury (35), and development of severe inflammation and lung fibrosis after bleomycin treatment (33). The findings of increased expression of *Mmp12* and *Mmp13* in M $\phi$  infected by *T. cruzi* (Fig. 5C and D) and in the heart tissue of chronically infected mice (Fig. 5H and I) in this study and in a previously published study (36) and increased MMP12 expression in infected M $\phi$  (Fig. 1G and H) suggest that these metalloproteinases may also play a key role in regulating pathological inflammation and fibrosis in CD. However, the mechanistic role of MMP12 and MMP13 in the context of CD was not addressed in this study or in previously published literature, and this remains to be examined in future studies.

The role of TGF- $\beta$  signaling in remodeling heart is complex and not completely understood. This is because its diverse effects elicit multiple and often opposing cellular responses. In brief, the TGF- $\beta$  superfamily transduces signal to downstream effectors primarily through the SMAD family of proteins, but it may also activate other signaling cascades, including extracellular signal-regulated kinase (Erk), c-Jun N-terminal kinase (JNK), TGF- $\beta$ -activated kinase 1 (TAK1), and p38 mitogen-activated protein kinase (MAPK) pathways (37, 38). Depending on the time, extent, and types of surface receptors and intracellular signaling cascades engaged, TGF- $\beta$  may play a crucial role in repression of the inflammatory response and mediate resolution of the inflammatory infiltrate after injuries caused by infectious or genotoxic stimuli (9). TGF- $\beta$  may be cardioprotective or play a key role as a mediator of pathological hypertrophy and ventricular remodeling, depending on the extent to which it modulates the fibroblast phenotype, promotes ECM deposition by upregulating collagen and fibronectin synthesis and by decreasing matrix degradation through induction of protease inhibitors, or stimulates cardiomyocyte growth and induces interstitial fibrosis (7, 39). In CD, TGF- $\beta$  is suggested to serve as a growth factor, promoting parasite replication (40), and treatment with a TGF- $\beta$  receptor inhibitor decreased the parasitemia, heart damage, and mortality in infected mice (41). Patients with the clinically symptomatic cardiac form of CD exhibit higher serum levels of TGF- $\beta$  than clinically asymptomatic seropositive patients, and CD patients with higher TGF- $\beta$  levels present a worse clinical outcome (42, 43). Our study showed significantly higher *Tgfb1* expression in the heart tissues of chronic CD-infected mice and *T. cruzi*-infected M $\phi$ . Thus, current literature and our data corroborate the importance of TGF- $\beta$  in the development and maintenance of cardiac damage in response to *T. cruzi* infection.

Besides its complex role, the unusual biology of TGF- $\beta$  activation is intriguing. Using a 3-dimensional collagen gel model loaded with TGF- $\beta$  in conjunction with fibroblasts deficient in MMP9, Kobayashi et al. (44) showed that MMP9 was required to activate TGF- $\beta$  and that MMP9 deficiency reduced the TGF- $\beta$ -driven responses, including activity of a *Smad3* reporter gene and production of fibronectin. Using TA3 murine mammary carcinoma cells, Yu and Stamenkovic (20) showed that MMP9 is localized on the

cell surface in a CD44-dependent manner and stimulates proteolytic cleavage of TGF- $\beta$ , and they proposed a novel role for MMP9 in TGF- $\beta$ -dependent tumorigenesis. Activation of TGF- $\beta$ 1 was at least partially dependent on MMP2 activity in age-associated arterial remodeling (45). TGF- $\beta$ , in turn, can inhibit MMP9 activity through the synthesis of protease inhibitors. Our data show that inhibition of MMP2, MMP9, or uPA (but not MMP12) abolished the M $\phi$  release of TGF- $\beta$  in response to *T. cruzi* infection. Whether MMP2 and MMP9 influence TGF- $\beta$  release through regulation of transcriptional, translational, or posttranslational activation programs in M $\phi$  infected by *T. cruzi* remains to be examined in future studies. Nonetheless, our findings provide the first evidence that during *T. cruzi* infection, M $\phi$  MMP9 plays a critical role in the activation of latent TGF- $\beta$  and that this in turn regulates cardiac fibroblast-to-myofibroblast differentiation.

PARP1 is widely regarded as an intracellular DNA damage sensor. In CD, innate immune cells responding to low-grade parasite persistence and mitochondrial dysfunction are recognized as major sources of free radicals (reviewed in references 2, 46, and 47), and the resultant oxidative DNA adducts were shown to cause PARP1 hyperactivation in cardiomyocytes and heart tissue infected by *T. cruzi* (21, 48). PARP1 direct binding and PARP1-mediated PARylation of proteins can affect the expression of inflammation-related genes at the transcriptional and posttranscriptional levels (21), and PARP1-dependent NF- $\kappa$ B-mediated proinflammatory gene expression was increased in cardiac myocytes infected by *T. cruzi* (48). Further, we have found that *T. cruzi* infection and chronic CD induce release of extracellular vesicles (EV) carrying oxidized DNA of host and parasite origin. When phagocytized by M $\phi$ , the oxidized DNA in these EV was sensed by the cytosolic DNA response element cGAS, which synergized with PARP1 to signal NF- $\kappa$ B transcriptional activation (12). Our results in this study show that *T. cruzi*-induced EV (TEV) were not profibrotic, and invasion by live *T. cruzi* was required to induce the MMP/TGF- $\beta$  expression in M $\phi$ . These findings suggest that TEV do not regulate the MMP and TGF- $\beta$  expression in M $\phi$  by the involvement of cytosolic cGAS-PARP1 and the downstream NF- $\kappa$ B signaling pathway. Instead, nuclear activation of Fos and JunB AP-1 transcription family proteins, in synergy with nuclear PARP1, signaled the increase in the expression and activity of MMP2, MMP9, and TGF- $\beta$  in M $\phi$  infected with *T. cruzi* (Fig. 7). This was evidenced by our findings in this study that genetic deletion or chemical inhibition of PARP1 abolished the *T. cruzi*-induced increase in mRNAs for *Mmp2*, *Mmp9*, *Mmp12*, and *Mmp13* in M $\phi$  and cardiac tissue of Chagas mice and decreased the expression of MMP9, TGF- $\beta$ , and profibrotic/fibrotic differentiation markers in heart tissue of CD-infected mice. Likewise, we reported previously that PJ34 (a PARP1 inhibitor) significantly improved the mitochondrial biogenesis and antioxidant capacity in the heart tissues of *T. cruzi*-infected mice and genetic deletion of PARP1 decreased the collagen deposition and the cardiac fibrosis and remodeling in chronically infected mice (49). Others have shown that treatment with olaparib (PARP1 inhibitor) ameliorated MMP2 and MMP9 expression in an elastase-induced mouse model of emphysema (50). Thus, based on our previous and present findings, we surmise that PARP1 plays an important role in progression of inflammation and fibrosis in CD through the engagement of cGAS-NF- $\kappa$ B and AP-1 signaling pathways.

MMP promoters harbor several *cis* elements, which allow the regulation of MMP gene expression by various transcriptional factors, such as AP-1, NF- $\kappa$ B, RUNX2, and STAT3, among others (reviewed in reference 22). PARP1 was shown to promote nuclear translocation of RelA (p65) in *T. cruzi*-infected cardiomyocytes (48) and to enhance NF- $\kappa$ B/AP-1 binding to the MMP9 promoter sequence in diabetic retinopathy (24) and JNK-dependent activation of AP-1 in murine fibroblasts (23). In this study, NF- $\kappa$ B only partially contributed to increases in *Mmp2* and *Mmp9* expression, and AP-1 was necessary to signal M $\phi$  expression of *Mmp2*, *Mmp9*, and *Tgfb1* in response to *T. cruzi* infection. Further, *Parp1*<sup>-/-</sup> (versus control) M $\phi$  exhibited significantly low activity of c-Fos and JunB AP-1 transcriptional family proteins. Our findings establish that PARP1 functions as a transcriptional coregulator of c-Fos and JunB members of the AP1 family

to drive the profibrotic/fibrotic response of M $\phi$ , and they offer novel insights into the role of PARP1 in the transcriptional regulation and release of M $\phi$  gelatinases and profibrotic TGF- $\beta$  in Chagas disease.

In summary, we used *in vitro* and *in vivo* models of *T. cruzi* infection and CD to show that M $\phi$  MMP2 and MMP9 released during *T. cruzi* infection are active and shape the ECM profibrotic response by the release of active TGF- $\beta$ . Chemical inhibition or genetic deletion of PARP1 arrested c-Fos- and JunB-mediated AP-1 transcriptional activation of MMP/TGF- $\beta$  responses in M $\phi$ , and this was beneficial in arresting the *T. cruzi*-driven cardiac fibroblast-to-myofibroblast differentiation in chronic CD. One limitation of the present study is that *Parp1*<sup>-/-</sup> mice express a shortened transcript lacking enzymatic activity in all cells and tissues, and it is possible that the observed decline in myocardial infiltration of profibrotic M $\phi$  and cardiac fibrosis in *Parp1*<sup>-/-</sup> mice was an outcome of the cumulative effects of PARP1 on AP-1–MMP9–TGF- $\beta$  signaling pathway (this study) and cGAS–NF- $\kappa$ B signaling of proinflammatory responses (our previous study [12]). Future studies in mice with M $\phi$ - and cardiomyocyte-specific knockdown of PARP1 will be needed to examine the relative importance of PARP1 signaling of cGAS–NF- $\kappa$ B and AP-1–MMP9–TGF- $\beta$  pathways in CD pathogenesis. Nevertheless, our findings make PARP1 an attractive target for CD therapy and provide an impetus for testing the efficacy of a variety of PARP1 inhibitors in controlling chronic inflammatory infiltrate and cardiac fibrosis, the two hallmarks of CD severity, in multiple mammalian hosts.

## MATERIALS AND METHODS

Six-week-old wild-type and *Parp1*<sup>-/-</sup> (both male and female) mice were infected with trypomastigotes of *T. cruzi* strain Sylvio X10 obtained from ATCC (10,000 parasites per mouse) and euthanized at ~150 days postinfection. RAW 264.7 (ATCC TIB-71), THP-1, and primary murine M $\phi$  and human cardiac fibroblasts (HCF) were cultured by standard protocols. Myocardial and splenic M $\phi$  were purified using the MagniSort mouse CD11b positive-selection kit. M $\phi$  were incubated with *T. cruzi* (cell-to-parasite ratio, 1:3), extracellular vesicles (EV) released from the infected cells, and/or various reagents for the time periods stated in the figure legends.

**Gene and protein expression.** Changes in the expression of target genes was examined by real-time RT-qPCR (22). Protein levels were determined by Western blotting. Zymography was performed to examine the release of MMP2 and MMP9 using Novex 10% Zymogram Plus gels following the manufacturer's instructions (Thermo Fisher Scientific). Images were analyzed by using ImageJ software. Quantitative ELISA was performed to monitor the release of active TGF- $\beta$ 1 (no. 88-8350; eBioscience), TNF- $\alpha$  (no. 88-7324; eBioscience), and MCP3/CCL7 (no. 205571; Abcam) in culture supernatants.

**Immunostaining.** HCF were incubated with spent cell culture supernatants of THP-1 M $\phi$  incubated with *T. cruzi* trypomastigotes and various inhibitors. Cells were sequentially incubated with anti-mouse S100A4 and rabbit anti-mouse alpha smooth muscle actin ( $\alpha$ -SMA) primary antibodies and fluorescence-conjugated secondary antibodies, and signals were analyzed on an Olympus BX-15 fluorescence microscope equipped with Simple PCI software (12).

Tissue sections were incubated with primary antibodies against CD68, TGF- $\beta$ , MMP9, galectin-3, and vimentin followed by horseradish peroxidase (HRP)- or allophycocyanin (AP)-conjugated secondary antibodies, and intensity and distribution of staining were scored as described previously (33).

**AP-1 transcriptional activity.** BM-derived primary M $\phi$  (WT and *Parp1*<sup>-/-</sup>) were incubated with *T. cruzi* and specific inhibitors, and AP-1 transcriptional activity was monitored using the 96-well TransAM AP-1 family transcription factor assay kit.

**Statistical analysis.** Data are presented as means and standard deviations (SD) ( $P < 0.05$ ). Details are given in the figure legends.

Detailed materials and methods are presented in Text S1.

## SUPPLEMENTAL MATERIAL

Supplemental material is available online only.

**TEXT S1**, DOCX file, 0.04 MB.

**FIG S1**, TIF file, 0.3 MB.

**FIG S2**, TIF file, 0.9 MB.

**FIG S3**, TIF file, 0.1 MB.

## ACKNOWLEDGMENTS

We are thankful to Nandadeva Lokugamage for breeding *Parp1*<sup>-/-</sup> mice and Imran Hussain Chowdhury for helping with the protocol for macrophage purification from cardiac tissues.

This work was supported by a grant from the National Institute of Allergy and Infectious Diseases (R01AI136031) of the National Institutes of Health to N.J.G. The funders had no role in study design, data collection and analysis, decision to publish, or preparation of the manuscript.

We declare no financial conflict of interest.

N.J.G. provided financial support and conceived and guided the study. S.C. performed the experiments, analyzed the data, and confirmed the reproducibility and accuracy of data presented in the manuscript. Both N.J.G. and S.C. wrote and edited the manuscript and approved the final version of the manuscript.

## REFERENCES

- Rios L, Campos EE, Menon R, Zago MP, Garg NJ. 2020. Epidemiology and pathogenesis of fetal-transplacental transmission of *Trypanosoma cruzi* and a case for vaccine development against congenital Chagas disease. *Biochim Biophys Acta Mol Basis Dis* 1866:165591. <https://doi.org/10.1016/j.bbadis.2019.165591>.
- Bonney KM, Luthringer DJ, Kim SA, Garg NJ, Engman DM. 2019. Pathology and pathogenesis of Chagas heart disease. *Annu Rev Pathol* 14:421–447. <https://doi.org/10.1146/annurev-pathol-020117-043711>.
- Acevedo GR, Girard MC, Gomez KA. 2018. The unsolved jigsaw puzzle of the immune response in Chagas disease. *Front Immunol* 9:1929. <https://doi.org/10.3389/fimmu.2018.01929>.
- Rios LE, Vazquez-Chagoyan JC, Pacheco AO, Zago MP, Garg NJ. 2019. Immunity and vaccine development efforts against *Trypanosoma cruzi*. *Acta Trop* 200:105168. <https://doi.org/10.1016/j.actatropica.2019.105168>.
- Tanowitz HB, Machado FS, Spray DC, Friedman JM, Weiss OS, Lora JN, Nagajyothi J, Moraes DN, Garg NJ, Nunes MCP, Ribeiro ALP. 2015. Developments in the management of Chagas cardiomyopathy. *Expert Rev Cardiovasc Ther* 13:1393–1409. <https://doi.org/10.1586/14779072.2015.1103648>.
- Machado FS, Dutra WO, Esper L, Gollob KJ, Teixeira MM, Factor SM, Weiss LM, Nagajyothi F, Tanowitz HB, Garg NJ. 2012. Current understanding of immunity to *Trypanosoma cruzi* infection and pathogenesis of Chagas disease. *Semin Immunopathol* 34:753–770. <https://doi.org/10.1007/s00281-012-0351-7>.
- Frangogiannis NG. 2019. The extracellular matrix in ischemic and non-ischemic heart failure. *Circ Res* 125:117–146. <https://doi.org/10.1161/CIRCRESAHA.119.311148>.
- Mouw JK, Ou G, Weaver VM. 2014. Extracellular matrix assembly: a multiscale deconstruction. *Nat Rev Mol Cell Biol* 15:771–785. <https://doi.org/10.1038/nrm3902>.
- Kong P, Christia P, Frangogiannis NG. 2014. The pathogenesis of cardiac fibrosis. *Cell Mol Life Sci* 71:549–574. <https://doi.org/10.1007/s00018-013-1349-6>.
- Medeiros NI, Gomes JAS, Correa-Oliveira R. 2017. Synergic and antagonistic relationship between MMP-2 and MMP-9 with fibrosis and inflammation in Chagas' cardiomyopathy. *Parasite Immunol* 39:e12446. <https://doi.org/10.1111/pim.12446>.
- Medeiros NI, Gomes JAS, Fiuza JA, Sousa GR, Almeida EF, Novaes RO, Rocha VLS, Chaves AT, Dutra WO, Rocha MOC, Correa-Oliveira R. 2019. MMP-2 and MMP-9 plasma levels are potential biomarkers for indeterminate and cardiac clinical forms progression in chronic Chagas disease. *Sci Rep* 9:14170. <https://doi.org/10.1038/s41598-019-50791-z>.
- Choudhuri S, Garg NJ. 2020. PARP1-cGAS-NFkB pathway of proinflammatory macrophage activation by extracellular vesicles released during *Trypanosoma cruzi* infection and Chagas disease. *PLoS Pathog* 16:e1008474. <https://doi.org/10.1371/journal.ppat.1008474>.
- Talvani A, Rocha MO, Barcelos LS, Gomes YM, Ribeiro AL, Teixeira MM. 2004. Elevated concentrations of CCL2 and tumor necrosis factor-alpha in chagasic cardiomyopathy. *Clin Infect Dis* 38:943–950. <https://doi.org/10.1086/381892>.
- Cunha-Neto E, Dzau VJ, Allen PD, Stamatidou D, Benvenuti L, Higuchi ML, Koyama NS, Silva JS, Kalil J, Liew C-C. 2005. Cardiac gene expression profiling provides evidence for cytokinopathy as a molecular mechanism in Chagas' disease cardiomyopathy. *Am J Pathol* 167:305–313. [https://doi.org/10.1016/S0002-9440\(10\)62976-8](https://doi.org/10.1016/S0002-9440(10)62976-8).
- Ho HH, Antoniv TT, Ji JD, Ivashkiv LB. 2008. Lipopolysaccharide-induced expression of matrix metalloproteinases in human monocytes is suppressed by IFN-gamma via superinduction of ATF-3 and suppression of AP-1. *J Immunol* 181:5089–5097. <https://doi.org/10.4049/jimmunol.181.7.5089>.
- Tang CH, Tsai CC. 2012. CCL2 increases MMP-9 expression and cell motility in human chondrosarcoma cells via the Ras/Raf/MEK/ERK/NF-kappaB signaling pathway. *Biochem Pharmacol* 83:335–344. <https://doi.org/10.1016/j.bcp.2011.11.013>.
- Gupta S, Garg NJ. 2015. A two-component DNA-prime/protein-boost vaccination strategy for eliciting long-term, protective T cell immunity against *Trypanosoma cruzi*. *PLoS Pathog* 11:e1004828. <https://doi.org/10.1371/journal.ppat.1004828>.
- da Costa AWF, do Carmo Neto JR, Braga YLL, Silva BA, Lamounier AB, Silva BO, Dos Reis MA, de Oliveira FA, Celes MRN, Machado JR. 2019. Cardiac Chagas disease: MMPs, TIMPs, galectins, and TGF-beta as tissue remodelling players. *Dis Markers* 2019:3632906. <https://doi.org/10.1155/2019/3632906>.
- Valiente-Alandi I, Schafer AE, Blaxall BC. 2016. Extracellular matrix-mediated cellular communication in the heart. *J Mol Cell Cardiol* 91:228–237. <https://doi.org/10.1016/j.yjmcc.2016.01.011>.
- Yu Q, Stamenkovic I. 2000. Cell surface-localized matrix metalloproteinase-9 proteolytically activates TGF-beta and promotes tumor invasion and angiogenesis. *Genes Dev* 14:163–176.
- Ba X, Gupta S, Davidson M, Garg NJ. 2010. *Trypanosoma cruzi* induces ROS-PARP-1-RelA pathway for up regulation of cytokine expression in cardiomyocytes. *J Biol Chem* 285:11596–11606. <https://doi.org/10.1074/jbc.M109.076984>.
- Fanjul-Fernandez M, Folgueras AR, Cabrera S, Lopez-Otin C. 2010. Matrix metalloproteinases: evolution, gene regulation and functional analysis in mouse models. *Biochim Biophys Acta* 1803:3–19. <https://doi.org/10.1016/j.bbamcr.2009.07.004>.
- Andreone TL, O'Connor M, Denenberg A, Hake PW, Zingarelli B. 2003. Poly(ADP-ribose) polymerase-1 regulates activation of activator protein-1 in murine fibroblasts. *J Immunol* 170:2113–2120. <https://doi.org/10.4049/jimmunol.170.4.2113>.
- Mishra M, Kowluru RA. 2017. Role of PARP-1 as a novel transcriptional regulator of MMP-9 in diabetic retinopathy. *Biochim Biophys Acta Mol Basis Dis* 1863:1761–1769. <https://doi.org/10.1016/j.bbadis.2017.04.024>.
- Gutierrez FRS, Lalu MM, Mariano FS, Milanezi CM, Cena J, Gerlach RF, Santos JET, Torres-Dueñas D, Cunha FQ, Schulz R, Silva JS. 2008. Increased activities of cardiac matrix metalloproteinases matrix metalloproteinase (MMP)-2 and MMP-9 are associated with mortality during the acute phase of experimental *Trypanosoma cruzi* infection. *J Infect Dis* 197:1468–1476. <https://doi.org/10.1086/587487>.
- Medeiros NI, Fares RCG, Franco EP, Sousa GR, Mattos RT, Chaves AT, Nunes MDCP, Dutra WO, Correa-Oliveira R, Rocha MOC, Gomes JAS. 2017. Differential expression of matrix metalloproteinases 2, 9 and cytokines by neutrophils and monocytes in the clinical forms of Chagas disease. *PLoS Negl Trop Dis* 11:e0005284. <https://doi.org/10.1371/journal.pntd.0005284>.
- Nosaka M, Ishida Y, Kimura A, Kuninaka Y, Inui M, Mukaida N, Kondo T. 2011. Absence of IFN-gamma accelerates thrombus resolution through enhanced MMP-9 and VEGF expression in mice. *J Clin Invest* 121:2911–2920. <https://doi.org/10.1172/JCI40782>.
- Robinson SC, Scott KA, Balkwill FR. 2002. Chemokine stimulation of monocyte matrix metalloproteinase-9 requires endogenous TNF-alpha. *Eur J Immunol* 32:404–412. [https://doi.org/10.1002/1521-4141\(200202\)32:2<404::AID-IMMU404>3.0.CO;2-X](https://doi.org/10.1002/1521-4141(200202)32:2<404::AID-IMMU404>3.0.CO;2-X).
- Quiding-Jarbrink M, Smith DA, Bancroft GJ. 2001. Production of matrix

- metalloproteinases in response to mycobacterial infection. *Infect Immun* 69:5661–5670. <https://doi.org/10.1128/iai.69.9.5661-5670.2001>.
30. Mouton AJ, Rivera Gonzalez OJ, Kaminski AR, Moore ET, Lindsey ML. 2018. Matrix metalloproteinase-12 as an endogenous resolution promoting factor following myocardial infarction. *Pharmacol Res* 137:252–258. <https://doi.org/10.1016/j.phrs.2018.10.026>.
  31. Bellac CL, Dufour A, Krisinger MJ, Loonchanta A, Starr AE, Auf Dem Keller U, Lange PF, Goebeler V, Kappelhoff R, Butler GS, Burtnick LD, Conway EM, Roberts CR, Overall CM. 2014. Macrophage matrix metalloproteinase-12 dampens inflammation and neutrophil influx in arthritis. *Cell Rep* 9:618–632. <https://doi.org/10.1016/j.celrep.2014.09.006>.
  32. Li H, Wang D, Yuan Y, Min J. 2017. New insights on the MMP-13 regulatory network in the pathogenesis of early osteoarthritis. *Arthritis Res Ther* 19:248. <https://doi.org/10.1186/s13075-017-1454-2>.
  33. Cabrera S, Maciel M, Hernández-Barrientos D, Calyeca J, Gaxiola M, Selman M, Pardo A. 2019. Delayed resolution of bleomycin-induced pulmonary fibrosis in absence of MMP13 (collagenase 3). *Am J Physiol Lung Cell Mol Physiol* 316:L961–L976. <https://doi.org/10.1152/ajplung.00455.2017>.
  34. Flechsig P, Hartenstein B, Teurich S, Dadrich M, Hauser K, Abdollahi A, Gröne H-J, Angel P, Huber PE. 2010. Loss of matrix metalloproteinase-13 attenuates murine radiation-induced pulmonary fibrosis. *Int J Radiat Oncol Biol Phys* 77:582–590. <https://doi.org/10.1016/j.ijrobp.2009.12.043>.
  35. Sen AI, Shiomi T, Okada Y, D'Armiento JM. 2010. Deficiency of matrix metalloproteinase-13 increases inflammation after acute lung injury. *Exp Lung Res* 36:615–624. <https://doi.org/10.3109/01902148.2010.497201>.
  36. Lokugamage N, Choudhuri S, Davies C, Chowdhury IH, Garg NJ. 2020. Antigen-based nano-immunotherapy controls parasite persistence, inflammatory and oxidative stress, and cardiac fibrosis, the hallmarks of chronic Chagas cardiomyopathy, in a mouse model of *Trypanosoma cruzi* infection. *Vaccines (Basel)* 8:96. <https://doi.org/10.3390/vaccines8010096>.
  37. Parichatikanond W, Luangmonkong T, Mangmool S, Kurose H. 2020. Therapeutic targets for the treatment of cardiac fibrosis and cancer: focusing on TGF-beta signaling. *Front Cardiovasc Med* 7:34. <https://doi.org/10.3389/fcvm.2020.00034>.
  38. Hu H-H, Chen D-Q, Wang Y-N, Feng Y-L, Cao G, Vaziri ND, Zhao Y-Y. 2018. New insights into TGF-beta/Smad signaling in tissue fibrosis. *Chem Biol Interact* 292:76–83. <https://doi.org/10.1016/j.cbi.2018.07.008>.
  39. Bujak M, Frangogiannis NG. 2007. The role of TGF-beta signaling in myocardial infarction and cardiac remodeling. *Cardiovasc Res* 74:184–195. <https://doi.org/10.1016/j.cardiores.2006.10.002>.
  40. Ming M, Ewen ME, Pereira ME. 1995. Trypanosome invasion of mammalian cells requires activation of the TGF beta signaling pathway. *Cell* 82:287–296. [https://doi.org/10.1016/0092-8674\(95\)90316-x](https://doi.org/10.1016/0092-8674(95)90316-x).
  41. Waghbi MC, de Souza EM, de Oliveira GM, Keramidas M, Feige J-J, Araújo-Jorge TC, Bailly S. 2009. Pharmacological inhibition of transforming growth factor beta signaling decreases infection and prevents heart damage in acute Chagas' disease. *Antimicrob Agents Chemother* 53:4694–4701. <https://doi.org/10.1128/AAC.00580-09>.
  42. Saraiva RM, Waghbi MC, Vilela MF, Madeira FS, Sperandio da Silva GM, Xavier SS, Feige JJ, Hasslocher-Moreno AM, Araujo-Jorge TC. 2013. Predictive value of transforming growth factor-beta1 in Chagas disease: towards a biomarker surrogate of clinical outcome. *Trans R Soc Trop Med Hyg* 107:518–525. <https://doi.org/10.1093/trstmh/trt050>.
  43. Araújo-Jorge TC, Waghbi MC, Hasslocher-Moreno AM, Xavier SS, Higuichi MDL, Keramidas M, Bailly S, Feige J-J. 2002. Implication of transforming growth factor-beta1 in Chagas disease myocardiopathy. *J Infect Dis* 186:1823–1828. <https://doi.org/10.1086/345882>.
  44. Kobayashi T, Kim H, Liu X, Sugiura H, Kohyama T, Fang Q, Wen F-Q, Abe S, Wang X, Atkinson JJ, Shipley JM, Senior RM, Rennard SI. 2014. Matrix metalloproteinase-9 activates TGF-beta and stimulates fibroblast contraction of collagen gels. *Am J Physiol Lung Cell Mol Physiol* 306:L1006–L1015. <https://doi.org/10.1152/ajplung.00015.2014>.
  45. Wang M, Zhao D, Spinetti G, Zhang J, Jiang L-Q, Pintus G, Monticone R, Lakatta EG. 2006. Matrix metalloproteinase 2 activation of transforming growth factor-beta1 (TGF-beta1) and TGF-beta1-type II receptor signaling within the aged arterial wall. *Arterioscler Thromb Vasc Biol* 26:1503–1509. <https://doi.org/10.1161/01.ATV.0000225777.58488.f2>.
  46. Lopez M, Tanowitz HB, Garg NJ. 2018. Pathogenesis of chronic Chagas disease: macrophages, mitochondria, and oxidative stress. *Curr Clin Microbiol Rep* 5:45–54. <https://doi.org/10.1007/s40588-018-0081-2>.
  47. Koo SJ, Garg NJ. 2019. Metabolic programming of macrophage functions and pathogens control. *Redox Biol* 24:101198. <https://doi.org/10.1016/j.redox.2019.101198>.
  48. Ba X, Garg NJ. 2011. Signaling mechanism of PARP-1 in inflammatory diseases. *Am J Pathol* 178:946–955. <https://doi.org/10.1016/j.ajpath.2010.12.004>.
  49. Wen JJ, Yin YW, Garg NJ. 2018. PARP1 depletion improves mitochondrial and heart function in Chagas disease: effects on POLG dependent mtDNA maintenance. *PLoS Pathog* 14:e1007065. <https://doi.org/10.1371/journal.ppat.1007065>.
  50. Dharwal V, Sandhir R, Naura AS. 2019. PARP-1 inhibition provides protection against elastase-induced emphysema by mitigating the expression of matrix metalloproteinases. *Mol Cell Biochem* 457:41–49. <https://doi.org/10.1007/s11010-019-03510-1>.